J Clin Periodontol 2004; 31: 534–544 doi: 10.1111/j.1600-051X.2004.00520.x
Printed in Denmark. All rights reserved

Journal of Clinical Periodontology

Histologic evaluation of demineralized freeze-dried bone allografts in barrier membrane covered periodontal fenestration wounds and ectopic sites in dogs

Morten Klepp[1], James E. Hinrichs[2], Ted Eastlund[3] and Erwin M. Schaffer[2]

[1]Private practice, Sola, Norway; [2]Department of Preventive Sciences, University of Minnesota School of Dentistry, Minneapolis, MN, USA; [3]Department of Lab Medicine and Pathology, University of Minnesota Medical School, Minneapolis, MN, USA

Klepp M, Hinrichs JE, Eastlund T, Schaffer EM: Histologic evaluation of demineralized freeze-dried bone allografts in barrier membrane covered periodontal fenestration wounds and ectopic sites in dogs. J Clin Periodontol 2004; 31: 534–544. doi: 10.1111/j.1600-051X.2004.00520.x. © Blackwell Munksgaard, 2004.

Abstract

Background/Aim: The aim of this study was to investigate healing responses to demineralized freeze-dried bone powder allografts in standardized periodontal fenestration defects, compared with subcutaneous wounds in a dog model.

Methods: Circular periodontal fenestration defects were created buccally at all four canines in 14 mongrel dogs. Each site received one of the following underneath a barrier membrane: (a) ethylene oxide (EO)-sterilized demineralized freeze-dried bone allografts (DFDBA), (b) heat-treated DFDBA, (c) non-sterilized DFDBA and (d) ungrafted control. Twelve of the 14 dogs had three subcutaneous chest wall pouches created and one of the three DFDBA materials placed in each. The animals were necropsied at 4 weeks. Histologic sections were prepared through the center of the fenestration sites in an apico-coronal direction. Quantitative analysis using computer-assisted imaging technique was performed. Subcutaneous implants were evaluated histologically and quantified for associated inflammatory cell infiltrate.

Results: Fenestration defects healed by partial osseous fill and cementum regeneration with formation of a periodontal ligament. The graft particles generally appeared isolated from the site of osteogenesis and covered by cementum-like substance. Graft particles incorporated into newly formed bone at a distance from the root surface was the exception. No statistically significant differences in new bone formation were observed between treatment groups within animals, but significant inter-animal variation was found ($p < 0.01$). Quantities of retained graft particles were limited, and without cellular resorption. A bone augmentation effect was associated with the barrier in the majority of sites. No bone formation was evident at the subcutaneous sites where graft particles displayed distinctly modified surface zones and multinucleated giant cell resorption. Significantly more inflammatory infiltrate was associated with EO-sterilized grafts compared with heat-treated grafts ($p = 0.05$).

Conclusion: Implantation of DFDBA neither enhanced osseous healing in periodontal fenestration defects, nor resulted in ectopic bone induction. DFDBA particles implanted in either periodontal fenestration or subcutaneous wounds evoked distinctly different healing responses.

Key words: barrier membrane; bone augmentation; bone induction; demineralized freeze-dried bone allograft; ethylene oxide; healing responses; pasteurization; periodontal fenestration wounds; sterilization processing

Accepted for publication 1 September 2003

Following the introduction of the bone induction principle (Urist 1965), with bone morphogenetic protein (BMP) as the identified inductive factor in bone matrix (Urist 1994), demineralized freeze-dried bone allografts (DFDBA) have been utilized and tested extensively for periodontal regeneration (Mellonig 1996). Histological evidence

of enhanced formation of bone, cementum and connective tissue attachment has been demonstrated in human periodontal defects (Bowers et al. 1989). However, other investigators have not been able to verify the effect of DFDBA on bone regeneration (Becker et al. 1994, Piattelli et al. 1996). Commercially available bone has been shown to induce variable amounts of ectopic bone in athymic mice (Becker et al. 1995) and in the rat bioassay (Schwartz et al. 1996).

To study experimentally the healing of periodontal structures, a model system has been advocated that predictably displays substantial regeneration to allow evaluation of tissue reaction and biologic potential (Wikesjö et al. 1994). The periodontal fenestration defect provides such a model, which offers the opportunity to study regeneration of alveolar bone, root cementum and connective tissue ligament in a standardized, well-defined wound unrelated to periodontal disease. The fenestration defect has been used to investigate the healing dynamics of the periodontium and the potential of bone derivatives and engineered materials to stimulate periodontal healing.

Barrier membranes have been utilized to protect and guide the healing of fenestration defects (Nalbandian & Helldén 1982, Nyman et al. 1982, Pettersson & Aukhil 1986, Caton et al. 1987). A standardized fenestration defect can be evaluated within the configuration of the cut surfaces of bone, periodontal ligament and root surface while covered by a barrier membrane. Caplanis et al. (1998a, b) found no histological effects following 4 weeks healing of DFDBA on bone activation in fenestration defects in maxillary canine teeth in beagle dogs, neither without or with a membrane covering the grafts. Nor did they find inflammatory cells associated with graft particles or evidence of resorption of the grafts.

Urist et al. (1967) demonstrated that heat treatment of the bone allograft material promoted bone induction in a large series of extraskeletal grafts. The highest incidence of bone formation after heating was noted with specimens heated to 40–60°C. The potential of heat to promote bone formation has later been repeated in an ectopic rat model (Morris 1978).

Studies examining the effect of ethylene oxide (EO) sterilization of DFDBA are inconclusive. Aspenberg and Lindqvist (1998) and Tshamala et al. (1999) found a decreased effect on bone induction following EO sterilization. However, effective osteoinduction has been demonstrated in rats following grafting with EO-sterilized DFDBA (Zhang et al. 1997), while similar healing was noted with EO-sterilized DFDBA as compared with autografts in the dog (Prolo et al. 1982). Consequently, sterilization processing or pasteurizing of the DFDBA material may influence the effectiveness of the graft to exert any biological activity. This has not been investigated in experimental, standardized periodontal defects.

The primary objectives of this investigation were to histologically examine the healing responses of periodontal fenestration defects grafted with EO-sterilized, heat-treated or non-sterilized DFDBA beneath barrier membranes as compared with ungrafted control sites beneath barriers. A secondary objective was to compare the healing characteristics of DFDBA embedded in ectopic sites in the animals and to contrast the response with those observed in the fenestration defects.

Materials and Methods

Fifteen adult mongrel dogs, 12 males and three females weighing 24–30 kg, were selected for this investigation. All animals initially had intact dentition with gingival status ranging from clinically healthy to moderately inflamed. No clinical evidence of periodontitis was detectable. All animal experimentation was conducted in accordance with the institutional Animal Care and Use Committee of the University of Minnesota. One dog was used in a pilot study.

Each animal was fasted the day prior to administration of anesthesia. A 5% dextrose solution with 30 mg/kg of sodium pentobarbital (60 mg/ml) was infused intravenously to induce anesthesia. Approximately 1.8–2.7 ml (36–54 mg) of Lidocaine 2% with 1/100,000 (0.018–0.027 mg) epinephrine was infiltrated locally.

Demineralized bone allografts and barrier material

Bone allograft material was obtained from American Red Cross Transplantation Services (St Paul, MN, USA). Donor cortical bone was procured from mongrel dogs. Processing procedures were in accordance with the American Association of Tissue Bank standards, including requirements for residuals of EO gas, percent residual moisture for freeze-dried bone powder and percent calcium for demineralized bone.

The powder allograft was divided into three groups. The first portion of the powder was placed in a dehydrater (Harvest Maid, Alternative Pioneering System Inc., Chaska, MN, USA) for 10 h at 60°C prior to being bottled and placed into the freeze drier (Virtis Consol 24, Virtis Co., Gardiner, NY, USA) and labeled heat-treated DFDBA bone (heat). The second portion was bottled and placed into the freeze drier and subsequently gas sterilized with EO. EO residues were removed according to the current standards. The third portion of bone powder, not secondarily sterilized (Non), was bottled in sterile bottles, and placed in the freeze drier.

An expanded polytetrafluoroethylene (ePTFE) membrane barrier (Gore-Tex Augmentation Material GTAM-4, W.L. Gore & Associates Inc., Flagstaff, AZ, USA) was used to cover all periodontal osseous defects including controls.

Surgical protocols

Periodontal fenestration lesions

The periodontal probing depth and width of attached gingiva over the facial aspect of all four canines in each animal were measured and compared. All visible plaque and calculus were removed with curettes. Following an initial horizontal incision within the attached gingiva a single releasing incision was made. A full-thickness flap was elevated over the canine root at approximately the junction of the coronal third and middle third of the root.

A trephine burr with an outer diameter of 8 mm was used to cut a standardized defect through the buccal facial bone. The exposed root surface was thoroughly planed to obtain a smooth surface. The trephine was used to secure a continuous notch around the circumference of the wounded root surface. The center of the circular exposed root surface was identified and notched with a #4 round burr, to a depth of approximately 1 mm (Fig. 1).

According to a pre-established protocol, each grafted defect was filled to exactly the level of the surrounding bone (Fig. 2). An ePTFE barrier membrane was trimmed to cover a minimum of 3 mm of bone adjacent to the defect

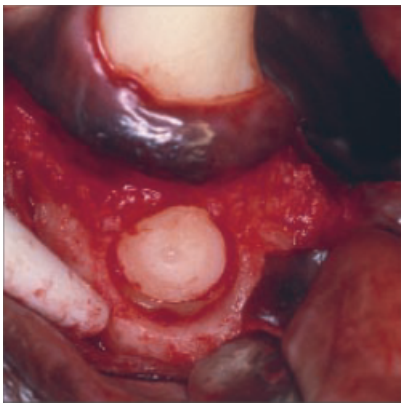

Fig. 1. Circular fenestration defect with peripheral and central notch.

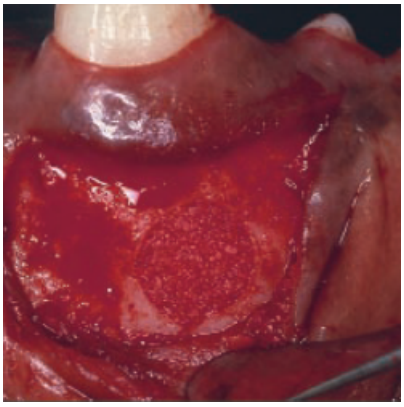

Fig. 2. Fenestration defect filled with demineralized freeze-dried bone allografts graft material.

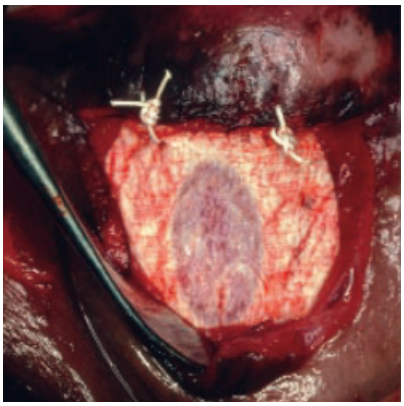

Fig. 3. Barrier membrane covering fenestration defect and adjacent bone, secured coronally with sutures.

in all directions and immobilized in position with two interrupted sutures to the attached gingiva (Fig. 3), prior to careful flap repositioning and wound closure by suturing (Gore-Tex 5-0 CV5, W.L. Gore & Associates Inc.). Control sites were prepared and covered identically to the experimental sites, but without graft material.

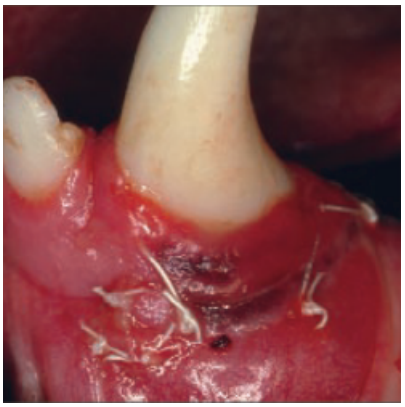

Fig. 4. Mandibular site following 4 weeks healing period.

The four periodontal fenestration sites in each animal received underneath the barrier either EO-sterilized DFDBA (EO), heat-treated DFDBA (Heat), non-sterilized DFDBA (Non) or no graft (Control). Distribution of the four treatments was rotated among animals.

Subcutaneous lesions

The right lateral chest wall of 12 animals was shaved and skin disinfected. Three vertical incisions separated by 6 cm were made in the skin of each animal. Lateral to each vertical incision a pouch was created into the loose subcutaneous tissue. A standardized quantity of 0.1 cm^3 of each of the DFDBA materials was delivered into one prepared site in each animal. Incisions were closed with sutures.

Post-operative care and healing phase

All animals were given an intramuscular injection of 300 000 U penicillin V. K. immediately after surgery and an equivalent daily dose for the subsequent 4 days.

Four weeks after the original surgery, the animals were anesthesized as previously described. Healing of the intraoral sites and skin incisions was evaluated clinically for sign of infection and closure of wound (Fig. 4). Any lack of flap closure or exposure, displacement or loss of membrane was recorded. The subcutaneous graft sites were identified by the healing incisions and by palpation of a firm mass beneath the skin.

Histologic procedures

Following euthanasia, block specimens including tooth, bone, membrane and overlying soft tissues were obtained. The fenestration block specimens were subjected to complete demineralization and subsequently sectioned in a plane perpendicular to the buccal root surface and parallel to the long axis of the root. The rounded central notch that had been placed during surgery was used as an orientation landmark. The tissue blocks were embedded in paraffin, sectioned at 4 µm and stained with hematoxylin and eosin (H&E). The soft tissue blocks were embedded in paraffin, sectioned at 4 µm and stained with H&E. All histological slides were coded and examined by two calibrated investigators who were blinded with respect to treatment groups and clinical findings.

One section per tooth, oriented through the central notch was selected for computer-assisted image analysis. The sections were quantitatively analyzed for: (1) total defect area (measured within the borders defined by the cut surfaces of existing coronal and apical alveolar bone, root surface including three notches, and inner aspect of covering membrane), (2) graft particle area within the defect and (3) new bone area within the defect. Multiple images were created for each histologic section. Area measurements were created as graphic overlay images traced by hand using a trackball controlled cursor on the monitor. All measurements were made once by the same calibrated investigator. Intra-examiner errors of identification and measurements were calculated by repeating the measurements on a randomly selected 10% sample of all sections, approximately 1 week after the initial measurements were taken. Intra-examiner reproducibility was $\pm$ 0.47% area new bone formation, and $\pm$ 0.03% area retained graft particles.

The subcutaneous implant specimens were examined for the presence, characteristics and distribution of graft particles in subcutaneous tissues. The inflammatory response associated with DFDBA particles was quantified using a scoring system from 0 to 3, indicating absence, mild, moderate and severe inflammatory infiltrate, respectively. In the case of conflicting scoring results between the two examiners, the mean value was calculated and employed for statistical analysis.

Statistical analysis

The statistical analysis was performed using a software program (SPSS/PC, SPSS Inc., Chicago, IL, USA). Image analysis of the areas of new bone and retained graft particles was expressed as a percentage of the total defect area. Square root transformation of the data was used for all statistical analysis. New bone formation and retained graft particles were compared within animals using paired *t*-tests and by analysis of variance (ANOVA). Differences between animals and treatment groups were tested by ANOVA. Non-parametric tests were performed because the assumption of normality can be questioned and the sample size was small for the central limit theorem to be invoked. The results were in accordance with the results of the parametric tests. Inflammatory infiltrate scores were compared between treatment groups within animals by Wilcoxon's signed-rank test.

Results

Clinical healing responses

The fenestration wounds displayed a range of clinical healing responses. Canine tooth graft sites with displacement or loss of membrane were recorded as failures. Graft sites with the membrane in place, but marginally exposed, apical to intact marginal periodontal tissues were recorded as exposures. The distribution of failures, exposures and completely healed sites, among treatment groups, is shown in

Table 1. Distribution of clinical failures, exposures and healed sites between canine treatment groups

Treatment group	Failures	Exposures	Complete healing
Control	3	3	8
EO	3	2	9
Non	3	2	9
Heat	5	3	6

Control, no graft; EO, EO-sterilized DFDBA; Non, non-sterilized DFDBA; Heat, heat-treated DFDBA; DFDBA, demineralized freeze-dried bone allografts; EO, ethylene oxide.

Table 1. Clinical healing of subcutaneous wounds was uneventful.

Histologic observations

Fenestration defects

Epithelial proliferation along the inner aspect of membrane or flap was observed in seven cases recorded as clinically healed. An inflammatory infiltrate was present in three of these cases. Six of 10 cases with clinically exposed membranes exhibited an extensive inflammatory infiltrate within the defect. However, for all cases in which a barrier was in place, these findings were evenly distributed between the four treatment groups.

The histological appearance in general was characterized by a well-integrated membrane, lack of inflammatory infiltrate, the presence of a small number of graft particles in the grafted defects, and the formation of woven bone extending from the osseous wound margins at varying distances. The histological characteristics of newly formed trabeculae associated with active bone formation and remodelling were identical in grafted (Fig. 5) and control specimens (Fig. 6), although bone fill displayed great variation. New bone trabeculae and graft particles were consistently separated from the root surface by a periodontal ligament space of normal width (Fig. 7). New cementum had in every case formed in one or both of the peripheral notches and frequently extended over the planed root surface, but the distance and thickness of cementum varied. A homogeneous layer of new cementum was most often seen extending from the wound periphery, following the apical/coronal notch outlines (Figs 5 and 8).

Graft particles were identified as rounded shapes of dense lamellar bone with empty lacunae. An abundance of graft particles was not characteristically present in the grafted defects. Foreign body cell reaction was not observed on or near graft particles, nor was osteoclastic resorption observed within the defects as defined by the membrane. In most cases, particles appeared isolated or in clusters within a connective tissue stroma, with a thin homogeneous surface layer of structure and staining characteristics similar to new cementum observed on the cut root surfaces. The homogenous surface layer was separated from the graft particle by a dark demarcation line (Fig. 9), and in some sections it was associated with scattered fibroblast-like cells while in other sections it was not associated with cells. In some specimens this homogenous layer bridged several particles together in a graft particle conglomerate (Figs 8 and 9). A union between particles and the root surface was seen in two specimens with continuity of the cementum-like layer of the particles and new root cementum. Polarized light microscopy displayed fiber orientation and structure of the surface layer distinctively different from the encapsulated graft particles (Fig. 10).

A well-defined cementum band within the central root notch was not observed at any site, but instead a characteristic ''tufting'', or coalescence of collagen fiber bundles perpendicular to the dentin surface was observed (Fig. 11).

Graft particles in several specimens were observed coronal to the defect, identified as separate particles and graft particle conglomerates (Fig. 8). In a few instances, a particle was identified buccal to the barrier (Fig. 12). These

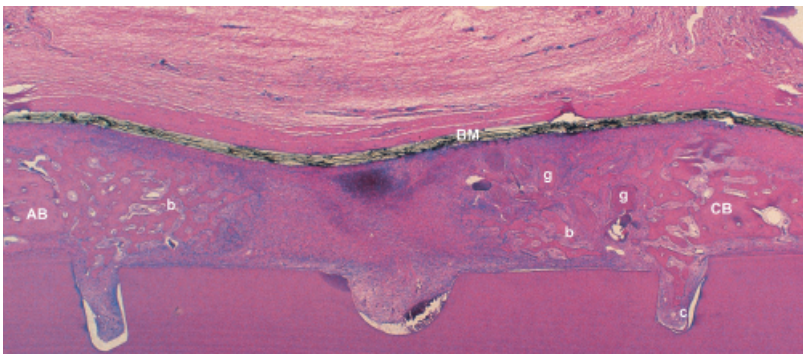

Fig. 5. Fenestration defect implanted with ethylene oxide-sterilized demineralized freeze-dried bone allografts (DFDBA) graft. Note 3 root notches. Barrier membrane (BM) is separating the osseous defect from the covering connective tissue. Note bordering apical alveolar (AB) and coronal alveolar bone (CB). A distinct band of new cementum (c) is identified in the coronal root notch, not in the apical notch. Graft particles (g) are present in the coronal aspect of the defect. New bone (b) trabeculae have formed extending from apical and coronal borders, and are seen extending towards the center, not closely associated with retained DFDBA particles (H&E stain, original magnification × 3.3).

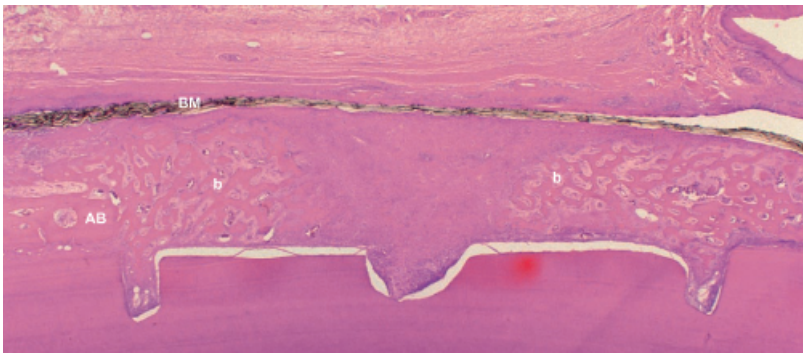

Fig. 6. Control defect. New bone formation (b) is extending towards center of defect from apical (AB) and coronal alveolar bone. Note barrier membrane (BM) in a convex shape over the osseous defect (H&E stain, original magnification × 3.3).

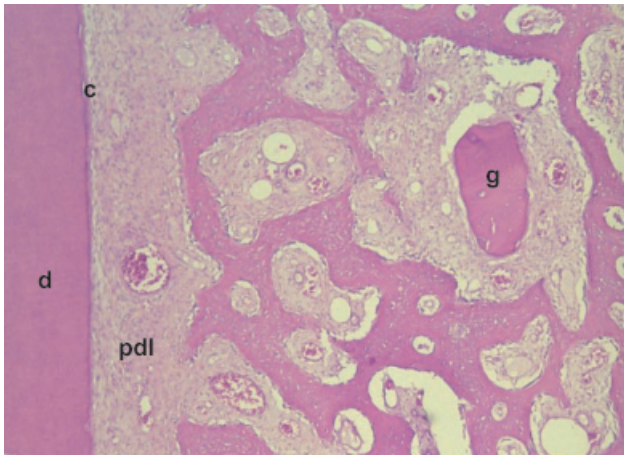

Fig. 7. Defect implanted witn non-sterilized graft. Particle (g) is separated from newly formed woven bone trabeculae by loose connective tissue. Note periodontal ligament space (pdl) separating actively forming bone, and dentin (d) covered by a thin layer of new cementum (c) (H&E stain, original magnification × 13.2).

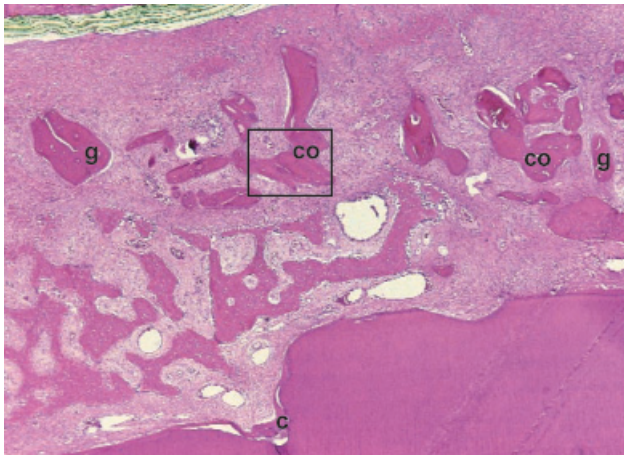

Fig. 8. Coronal border of defect implanted with ethylene oxide-sterilized graft. Coronal root notch is partially filled with new cementum (c). Note conglomerates of graft particles (co) embedded in cementum-like substance (H&E stain, original magnification × 10).

particles failed in every case to display cementum-like layer on surface and was identified with multinucleated giant cells in resorption lacunae (Fig. 13).

Exceptions to these predominant healing characteristics were observed in three defects in one of three animals, grafted with heat-, EO- and non-sterilized DFDBA, respectively. Bone formation in these sections was identified in direct contact with some of the graft particles at a distance from the root surface toward the membrane, while other particles appeared isolated. Complete encapsulation of graft particles was observed, resulting in amalgamation of particles and repair bone. In three additional specimens this amalgamation was observed coronal to the experimental defect (Figs 12 and 14).

Table 2. Osseous augmentation associated with barrier membrane. Frequency distribution

Treatment group	Buccal osseous augmentation/total number of sites
Control	5/11
Heat	8/9
EO	9/11
Non	9/11

Control, no graft; EO, EO-sterilized DFDBA; Non, non-sterilized DFDBA; Heat, heat-treated DFDBA; DFDBA, demineralized freeze-dried bone allografts; EO, ethylene oxide.

Formation of bone within the defect occurred in most specimens buccally to the width of remaining intact bone beyond the edge of the fenestration, and was limited by the membrane (Fig. 12). Further, the membrane frequently displayed a buccal bulging over the central portion of the defect (Fig. 6). Osteoblastic activity and trabeculation was observed on the buccal aspect of intact adjacent alveolar bone where periosteum had been surgically elevated and the denuded bone covered by membrane. This buccal bone augmentation was histologically associated with the degree of membrane overlap and the space provided by it. A frequency distribution of buccal augmentation among treatment groups is shown in Table 2.

Subcutaneous lesions

Histologic sections were obtained from 34 of a total of 36 grafted lesions. The graft particles were retained in close proximity most often surrounded by a collagenous capsule, isolated from loose connective tissue, glandular structures and covering epithelium. Microabscesses were infrequent and were apparently not associated with the implant material. In close proximity with the clustered graft particles were inflammatory cell infiltrates of varying intensity between specimens. Cells were

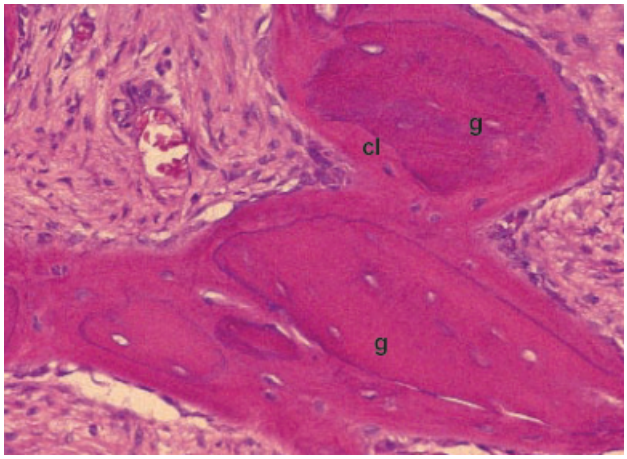

Fig. 9. Detail from Fig. 8, graft particle conglomerate. Note cellular cementum-like substance (cl) embedding graft particles (g) with empty lacunae (H&E stain, original magnification × 40).

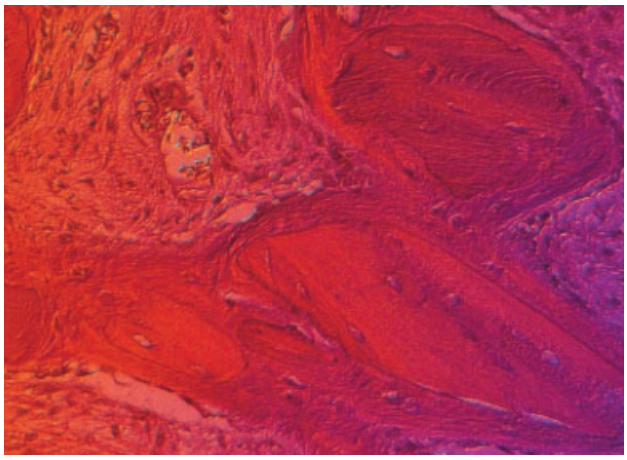

Fig. 10. Graft particle conglomerate in Fig. 9, photographed using Nomarski filters. Note fiber directions in cementum-like substance differing from lamellae pattern in graft particles (H&E stain, original magnification × 40).

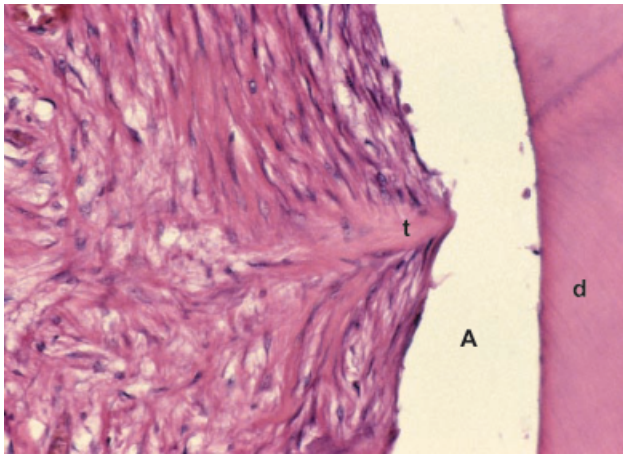

Fig. 11. Coalesence of collagen fiber bundles, ''tufting'' (t), perpendicular to the dentin (d) surface within the central notch. Artifactual tissue separation (A) (H&E stain, original magnification × 80).

predominantly mononuclear monocytes/macrophages, and multinucleated giant cells were common. Lymphocytes and plasma cells were less abundant. Multinucleated giant cells were contiguous to graft particles in all specimens (Figs 15–18).

On the surface of graft particles in all treatment groups, a narrow zone of relatively constant width, taking a lighter stain, was observed (Figs 15–17). A dark line resembling a resting line demarcated this peripheral zone of the particle core. Flattened cells were scattered on the surface of occasional graft particles, and osteocyte lacunae were empty in all specimens. On graft particles with well-defined osteons, the lamellae could be followed through the particle surface zone, to the periphery of the particle when using polarized light filters and Nomarski optics (Figs 17 and 18). Fiber bundles oriented independently could not be detected in the surface zones. One additional specimen containing DFDBA graft implanted 2 h prior to euthanasia failed to display lighter surface zones.

Histometric analysis

Fenestration lesions

Prior to statistical analysis a total of 14 sites were removed because of loss or displacement of barrier membrane, disrupting the balanced distribution of treatment groups. The number of exposed cases was too small for statistical testing to be performed. Since the results were not consistently influenced in any direction, and because excluding exposed sites resulted in a sample size too small to make statistical inferences, data from all image-analyzed sections were included in the statistical tests. While the use of two-way ANOVA is not completely justified, the ANOVA results are presented as a practical overview of the results. Additional analysis using paired *t*-tests and non-parametric tests confirmed the ANOVA results.

No significant differences in bone formation between treatment groups occurred (Table 3), but statistically significant inter-animal variation in osseous regeneration was demonstrated ($p < 0.01$). The percentage retained graft particles was dependent upon treatment, when comparing grafted sites and control sites ($p < 0.05$) with no significant inter-animal variation (Table 4). No statistically significant correlation ex-

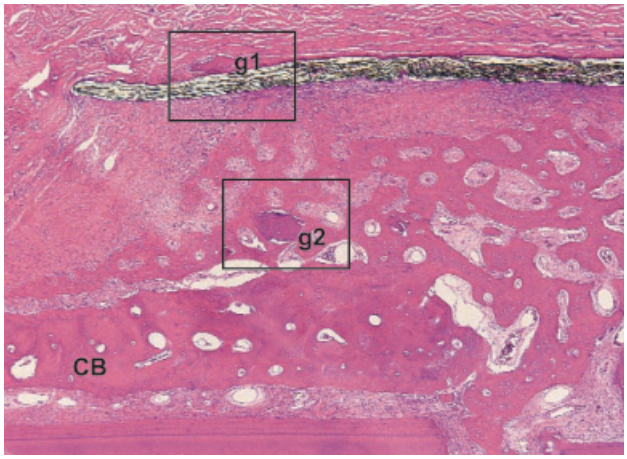

Fig. 12. Coronal aspect of defect implanted with ethylene oxide-sterilized graft. Note graft particle (g1) displaced buccally to barrier, and graft particle (g2) embedded within augmented bone. Coronal extension of buccal bone augmentation is associated with barrier membrane overlap (H&E stain, original magnification × 10).

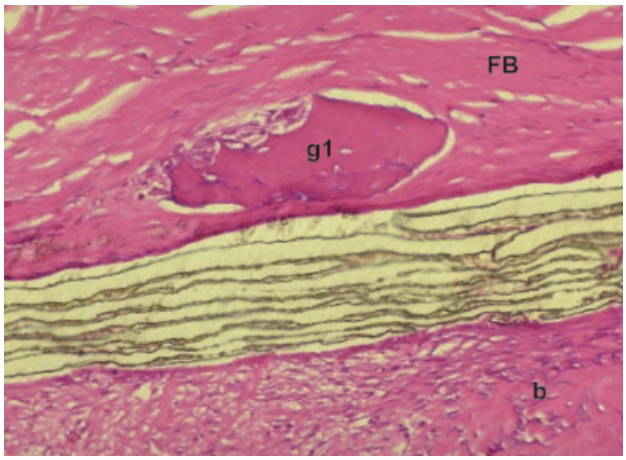

Fig. 13. Detail of ethylene oxide-sterilized particle (g1) in Fig. 12. The particle is identified buccally to barrier membrane, embedded in collagen fiber bundles (FB). Multinucleated giant cells are present within resorption lacunae. Note absence of cellular inflammatory infiltrate associated with particle, and proximity to early bone formation (b) on inner aspect of barrier membrane (H&E stain, original magnification × 50).

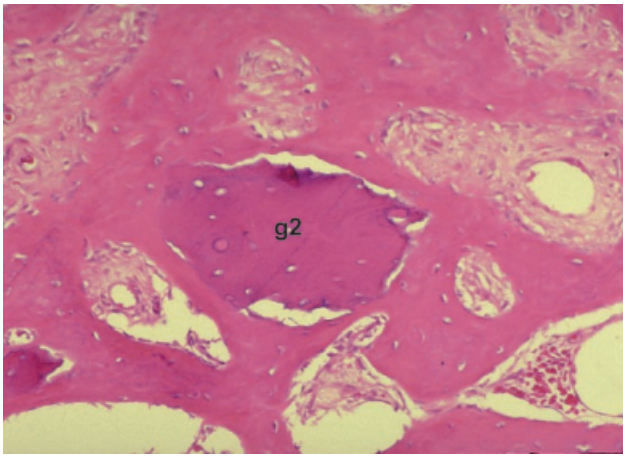

Fig. 14. Detail of ethylene oxide-sterilized particle (g2) in Fig. 12. Particle is clearly identified by empty osteocyte lacunae and cortical lamellar pattern. It is embedded in newly formed bone without intermediate soft tissue, with no cementum-like substance on particle (H&E stain, original magnification × 50).

isted between amounts of new bone formation and retained graft particles.

Subcutaneous lesions

Sites grafted with EO-sterilized DFDBA demonstrated the largest variation in inflammatory infiltrate score, ranging from absence to severe inflammatory infiltrate. There was significantly less inflammatory infiltrate associated with heat-treated grafts when compared with EO-sterilized grafts ($p = 0.05$) (Table 5).

Discussion

Several investigators have studied periodontal regeneration using rectangular-shaped fenestrations of a defined size (Caton et al. 1987, Choi et al. 1993, Caplanis et al. 1998a, b). The use of critical sized, surgically created bony defects have been advocated (Schmitz & Hollinger 1986) to study bone regeneration. In the present study, the defect shape and size was selected based on canine root morphology and data on healing of mongrel dog jaw defects. Mandibular 5 mm trephine defects through the buccal cortical plate in mongrel dogs have previously shown complete osseous regeneration, whereas 8 mm defects showed healing by fibrous tissue and partial osseous fill after 16 weeks (Hjørting-Hansen & Andreasen 1971). Complete healing of trephine fenestrations in the presence of barrier depends more upon post-operative healing time than defect size according to the results of osseous regeneration obtained in monkeys (Dahlin et al. 1990) and in dogs (Caplanis et al. 1998b) using the principle of guided tissue regeneration. Results from our pilot study supported the choice of an 8 mm defect in conjunction with the placement of membrane and an evaluation after a 4-week healing period.

Bone exhibits the most complex spectrum of growth factor activities of any tissue (Hauschka et al. 1988, Mohan & Baylink 1991), and surgical trauma to bone releases circulating factors (Einhorn et al. 1990) able to interact with the surrounding determined osteogenic precursor cells and the inducible precursor cells found in ectopic sites (Friedenstein 1973). It has been suggested (Schenk 1994) that the term bone induction be replaced by bone activation in the healing of bony lesions.

The present study demonstrates bone activation, evident as osseous healing

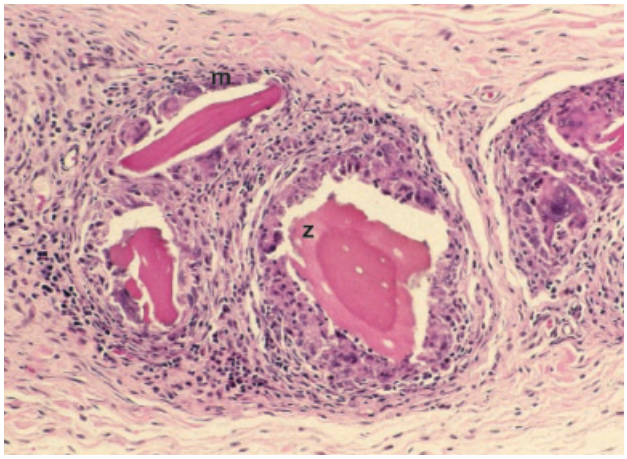

Fig. 15. Subcutaneous implantation site. Ethylene oxide-sterilized graft particles are associated with severe inflammatory infiltrate. Note the well-demarcated surface zone (z) on larger particle. Graft particles are undergoing resorption by multinucleated giant cells (m) (H&E stain, original magnification × 50).

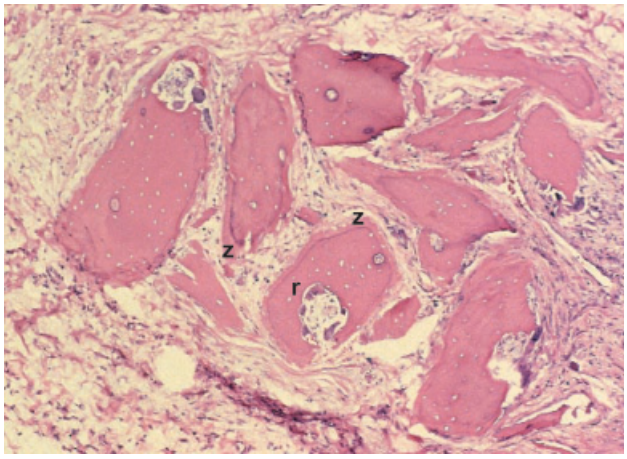

Fig. 16. Subcutaneous implantation site. Heat-treated graft particles are associated with mild inflammatory infiltrate. Note multinucleated giant cells within resorption lacunae (r) and a lighter, narrow surface zone (z) on several particles (H&E stain, original magnification × 25).

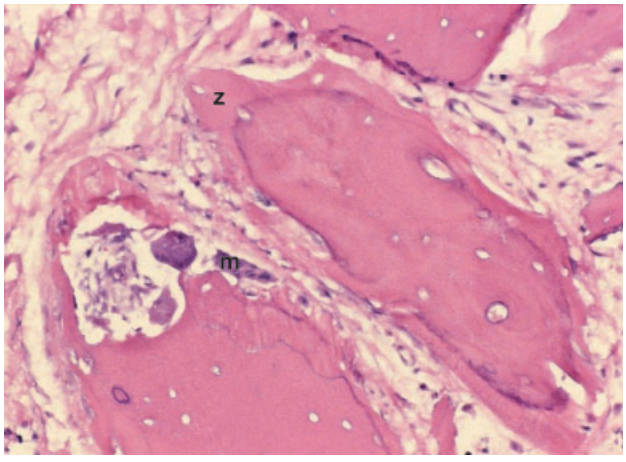

Fig. 17. Higher magnification of particles in Fig. 16. Note empty lacunae, surface zones (z) and multinucleated giant cells (m) associated with the surface zone on a particle (H&E stain, original magnification × 66).

extending from the osseous wound margins to a varying extent in all treatment groups. This has previously been demonstrated by others in fenestration defects both with (Scopp et al. 1966, Choi et al. 1993, Caplanis et al. 1998a), and without (Caton et al. 1987) bone graft placement.

No differences in osseous healing were found between controls and grafted sites, but a significant variation in osseous fill existed between animals, demonstrating that the individual dog was the critical factor rather than treatment with bone grafting. Variable release of and response to osteogenic factors may have contributed to this animal-dependent new bone formation, and lack of differences between treatments. Any bone activation effect from implanted DFDBA material may have been insignificant compared with impact from autogenous factors. Studies have shown wide variation in the ability of commercial bone bank DFDBA to induce bone formation (Schwartz et al. 1996, 1998a) due to differences in BMP content from individual donors. Although the DFDBA material in this study was prepared using pooled bones from several donor dogs, the level of osteogenic factors in grafts delivered to the surgical sites was not controlled.

The frequent observation of enhanced bone apposition on the outer aspect of existing alveolar bone with grafting indicates that placement of a filler graft acts to provide and maintain a space for the healing process. However, few particles were retained within the defects at 4 weeks. Despite implantation of the well-adapted barrier membrane between the graft and overlying flap, it appears likely that a substantial number of particles have leaked from the created fenestration. This is indicated by the occasional finding of graft particles buccal to barrier membrane and buccal to coronal alveolar bone. The wide and shallow configuration of the defects would possibly lend themselves to greater chances of implant particle loss, despite the use of a barrier, than would deeper and narrower defects. Correlation testing failed to show statistically significant correlation between new bone and retained graft particles. This is in concordance with the majority of retained DFDBA particles appearing isolated from active osteogenesis in the present study, but is contrasted to the findings in human intra-bony defects where defects harbor-

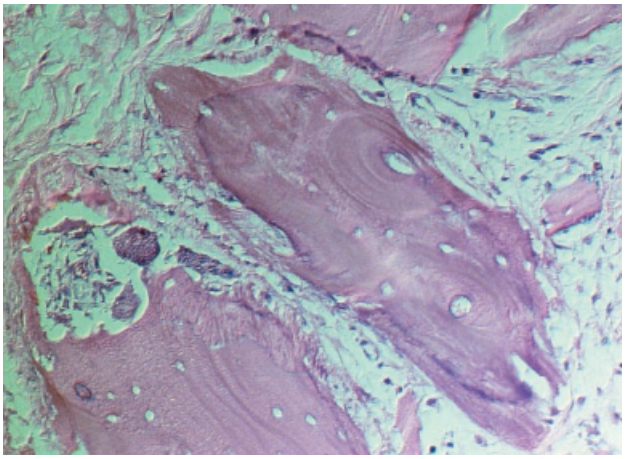

Fig. 18. Graft particles in Fig. 17, photographed using Nomarski filters. Lamellar patterns and fiber bundle directions can be followed through the surface zones (H&E stain, original magnification × 66).

Table 3. New bone formation by treatments and dogs, excluding failures

Source of variation	Sum of squares	Degrees of freedom	Mean square	*p*
treatment	0.14	3	0.05	>0.1
dog identity	65.86	13	5.07	0.003
residual	35.47	25	1.42	

ANOVA, analysis of variance. Square root transformed scale.

Table 4. Retained graft particles by treatments and dogs, excluding failures

Source of variation	Sum of squares	Degrees of freedom	Mean square	*p*
treatment modality	5.41	3	1.81	0.04
dog identity	5.49	13	0.42	>0.1
residual	13.73	25	0.55	

ANOVA, analysis of variance. Square root transformed scale.

Table 5. Comparisons of inflammatory infiltrate scores between pairs of treatment groups within animals

X	*Y*	*N*	*X*⩾*Y*	*p*
Treatments				
EO	Heat	11	10	0.05
EO	Non	11	7	>0.1
Non	Heat	10	8	<0.1

Wilcoxon's matched pairs signed-rank test. EO, EO-sterilized DFDBA; Non, non-sterilized DFDBA; Heat, heat-treated DFDBA; DFDBA, demineralized freeze-dried bone allografts; EO, ethylene oxide.

ing residual graft particles exhibited significantly greater amounts of new bone and cementum formation, compared with defects without evident grafts after 6 months of healing (Reynolds and Bowers 1996).

The DFDBA particles grafted in fenestration defects evoked different healing responses. The appearance of particles generally separated by a zone of less organized connective tissue is in agreement with the findings in grafted human extraction sockets (Becker et al. 1994), while sections from six fenestration sites representing all three grafting modalities displayed amalgamation or embedding of particles. Similar embedding patterns have been reported with DFDBA in rat mandibular defects (Glowacki et al. 1981) and in human intra-bony defects (Reynolds and Bowers 1996), and were further reported with viable and non-viable intra-oral autogenous bone in furcations (Ellegaard et al. 1975) as well as with defatted, chemically sterilized and lyophilized bovine bone in fenestration defects (Scopp et al. 1966) in monkeys.

In the present study, a distinct band of cementum-like substance on particle surfaces was the dominant finding. This characteristic has been described by several investigators and has been demonstrated on intra-oral autografts (Ellegaard et al. 1975), and bovine xenografts (Nielsen et al. 1980) in monkeys. The presence of bands of newly formed matrix has previously been termed new bone formation with osteoblasts on autogenous dentin and cementum implants in dog and monkey (Schaffer 1957) and on DFDBA in humans (Bowers et al. 1985, 1989).

The width of the cementum-like layer on graft particles observed in the present investigation was consistent and comparable with new cementum formed on the root surfaces. The cementum-like layer was in proximity of cells that were morphologically similar to cementoblasts and exhibited staining characteristics consistent with cementoblasts associated with newly formed cementum. Polarized light microscopy strongly suggests the layer was formed de novo on implanted particles. The matrix appeared without active formation at 4 weeks post-implantation, in contrast to the surrounding actively forming bone trabeculae. The differences in matrix quantity and quality as well as cellular differences between particle surface zones and bone trabeculae preclude identifying the particle matrix as osseous regeneration.

If a specific cell population was responsible for cementum regeneration (Melcher 1976), the particles at some distance away from intact periodontal ligament space would not be expected to display this surface zone. However, the presence of cementum-like material on graft particles was not dependent upon their proximity with the periodontal ligament space (Fig. 8), suggesting that cells both from periodontal ligament and bone, dividing and migrating into the wound at equal pace (Iglhaut et al. 1988), are responsible for the cementum-like substance. In vitro studies showing synthesis of cementum-like tissue by cells cultured from bone (Melcher et al. 1986) add support to the involvement of osseous tissue in this repair process. In every case where bone graft particles were observed ectopically on the buccal aspects of the barrier, the particles failed to display any cementum-like modification on the surface. This observation supports the theory that this matrix is derived from cells of bone or periodontal ligament compartments.

DFDBA particles implanted in subcutaneous sites evoked distinctively different responses compared with the

fenestration defects. The inert appearances at periodontal sites were contrasted by the presence of active multinuclear-giant cell resorption and varying degrees of inflammatory cellular infiltrate, without ectopic bone formation.

Both EO sterilized, heat-treated and non-sterilized DFDBA typically displayed demarcated and modified surface zones, although this was not present on every particle in the sections. An eosinophilic zone with decreased density and distinguishable fiber pattern was noted on the periphery of the graft particles, suggesting a portion of the demineralized matrix had been removed during early healing. The multinucleated giant cells were most frequently present in distinct resorption lacunae without an intermediate eosinophilic surface zone, indicating that surface layer modification and multinucleated giant cell resorption may be separate processes. The eosinophilic surface zones were not present on particles in a 2-h specimen, suggesting the distinct zones represent a surface modification of the particles following subcutaneous implantation.

While DFDBA particles appeared inert in the barrier-protected periodontal osseous sites, being encapsulated at 4 weeks in matrix produced by determined osteogenic precursor cells, the subcutaneously placed particles were subjected to cellular resorption and inflammatory responses, apparently unable to activate inducible precursor cells to form bone. The degree of particle demineralization during DFDBA processing has been shown to be of importance for osteoclastic resorption in vitro (Herold et al. 2002), which is suggested to be of importance to further unmask the bone morphogenetic fraction and induce bone formation. This is not substantiated by the present results as no bone induction was observed. Other investigations strongly indicate that bioactive substances of known activity must be added to DFDBA to achieve osteoinductivity (Bowers et al. 1991, Schwartz et al. 1998b).

A striking finding in our study is the differences in healing responses, to the EO-sterilized DFDBA particles in particular. The statistically significant difference in inflammatory infiltrate associated with extraskeletally implanted DFDBA, between EO-sterilized and heat-treated grafts, suggests a relationship to EO residues in the allograft. However, EO-sterilized particles in the fenestration defects evoked identical responses compared with heat-treated and non-sterilized grafts, without inflammatory infiltrate. Previous studies have shown the toxic effect that residual EO gas has in vitro for gingival fibroblasts (Kudryk et al. 1992); EO-sterilized bone–patellar tendon–bone allografts have (Jackson et al. 1990, Roberts et al. 1991) and have not (Noyes et al. 1990) been associated with a higher inflammatory cell infiltrate in humans. In our study, the inflammatory score varied from absence to severe for the EO-sterilized ectopic grafts. Whereas the differences between the studied tissue compartments, cellular populations and surgical wounds are obvious, no further explanation is suggested why the animals appeared to accept the implant in one part of the body and not in another, and why this appeared most pronounced for EO-sterilized DFDBA.

Acknowledgments

This article was supported by the American Red Cross, W. L. Gore & Associates Inc., the Schaffer Research Chair and the Periodontal Research Center, University of Minnesota. The authors gratefully acknowledge Dr Knut A. Selvig for advice in the preparation of this paper.

References

Aspenberg, P. & Lindqvist, S. B. (1998) Ethylene oxide and bone induction. Controversy remains. *Acta Orthopaedica Scandinavia* **69**, 173–176.

Becker, W., Becker, B. E. & Caffesse, R. (1994) A comparison of demineralized freeze-dried bone and autologous bone to induce bone formation in human extraction sockets. *Journal of Periodontology* **65**, 1128–1133.

Becker, W., Urist, M. R., Tucker, L. M., Becker, B. E. & Oschenbein, C. (1995) Human demineralized freeze-dried bone: inadequate induced bone formation in athymic mice. A preliminary report. *Journal of Periodontology* **66**, 822–828.

Bowers, G. M., Chadroff, B., Carnevale, R., Mellonig, J., Corio, R., Emerson, J., Stevens, M. & Romberg, E. (1989) Histologic evaluation of new attachment apparatus formation in humans. Part III. *Journal of Periodontology* **60**, 683–693.

Bowers, G. M., Granet, M., Stevens, M., Emerson, J., Corio, R., Mellonig, J., Lewis, S. B., Peltzman, B., Romberg, E. & Risom, L. (1985) Histologic evaluation of new attachment in humans. A preliminary report. *Journal of Periodontology* **56**, 381–396.

Bowers, G. M., Felton, F., Middleton, C., Glynn, D., Sharp, S., Mellonig, J. T., Corio, R., Emerson, J., Park, S., Suzuki, J., Ma, S., Romberg, E. & Reddi, A. H. (1991) Histologic comparison of regeneration in human intrabony defects when osteogenin is combined with demineralized freeze-dried bone allograft and with purified bovine collagen. *Journal of Periodontology* **62**, 690–702.

Caplanis, N., Lee, M. B., Zimmerman, G. J., Selvig, K. A. & Wikesjö, U. M. E. (1998a) Effect of allogenic freeze-dried demineralized bone matrix on regeneration of alveolar bone and periodontol attachment in dogs. *Journal of Periodontology* **25**, 801–806.

Caplanis, N., Lee, M. B., Zimmerman, G. J., Selvig, K. A. & Wikesjö, U. M. E. (1998b) Effect of allogenic freeze-dried demineralized bone matrix on guided tissue regeneration in dogs. *Journal of Periodontology* **69**, 851–856.

Caton, J. G., DeFuria, E. L., Polson, A. M. & Nyman, S. (1987) Periodontal regeneration via selective cell repopulation. *Journal of Periodontology* **58**, 546–552.

Choi, S. Y., Nilvéus, R. E., Minutello, R. D., Zimmerman, G. J. & Wikesjö, U. M. E. (1993) Effect of a collagen matrix on healing in periodontal fenestration defects in dogs. *Journal of Periodontology* **64**, 878–882.

Dahlin, C., Gottlow, J., Linde, A. & Nyman, S. (1990) Healing of maxillary and mandibular bone defects using a membrane technique. An experimental study in monkeys. *Scandinavian Journal of Plastic and Reconstructive Surgery and Hand Surgery* **24**, 13–19.

Einhorn, T. A., Simon, G., Devlin, V. J., Warman, J., Sidhu, S. P. S. & Vigorita, V. J. (1990) The osteogenic response to distant skeletal injury. *Journal of Bone and Joint Surgery – American Volume* **72A**, 1374–1378.

Ellegaard, B., Karring, T. & Löe, H. (1975) The fate of vital and devitalized bone grafts in the healing of interradicular lesions. *Journal of Periodontal Research* **10**, 88–97.

Friedenstein, A. J. (1973) Determined and inducible osteogenic precursor cells. In: *Hard Tissue Growth Repair, and Remineralization, Ciba Foundation Symposium* **11**, eds Elliot, K & Fitzsimmons, D., pp. 169–185. Amsterdam: Elsevier.

Glowacki, J., Kaban, L. B., Murray, J. E., Folkman, J. & Mulliken, J. B. (1981) Application of the biological principle of induced osteogenesis for craniofacial defects. *Lancet* **1**, 959–963.

Hauschka, P., Chen, T. & Mavrakos, A. (1988) Polypeptide growth factors in bone matrix. *Ciba Foundation Symposium* **136**, 207–225.

Herold, R. W., Pashley, D. H., Cuenin, M. F., Niagro, F., Hokett, S. D., Peacock, M. E., Mailhot, J. & Borke, J. (2002) The effects of varying degrees of allograft decalcification on cultured porcine osteoclast cells. *Journal of Periodontology* **73**, 213–219.

Hjørting-Hansen, E. & Andreasen, J. (1971) Incomplete bone healing of experimental

cavities in dog mandibles. *British Journal of Oral Surgery* **9**, 33–40.

Iglhaut, J., Aukhil, I., Simpson, D. M., Johnston, M. C. & Koch, G. (1988) Progenitor cell kinetics during guided tissue regeneration in experimental periodontal wounds. *Journal of Periodontal Research* **23**, 107–117.

Jackson, D. W., Windler, G. E. & Simon, T. M. (1990) Intraarticular reaction associated with the use of freeze-dried, ethylene oxide-sterilized bone-patella tendon-bone allografts in the reconstruction of the anterior cruciate ligament. *American Journal of Sports Medicine* **18**, 1–11.

Kudryk, V. L., Scheidt, M. J., McQuade, M. J., Sutherland, D. E., Van Dyke, T. E. & Hollinger, J. O. (1992) Toxic effect of ethylene-oxide-sterilized freeze-dried bone allograft on human gingival fibroblasts. *Journal of Biomedical Materials Research* **26**, 1477–1488.

Melcher, A. H. (1976) On the repair potential of periodontal tissues. *Journal of Periodontology* **47**, 256–260.

Melcher, A. H., Cheong, T., Cox, J., Nemeth, E. & Shiga, A. (1986) Synthesis of cementum-like tissue in vitro by cells cultured from bone: a light and electron microscope study. *Journal of Periodontal Research* **21**, 592–612.

Mellonig, J. T. (1996) Bone allografts in periodontal therapy. *Clinical Orthopaedics and Related Research* **324**, 116–125.

Mohan, S. & Baylink, D. J. (1991) Bone growth factors. *Clinical Orthopaedics and Related Research* **263**, 30–48.

Morris, M. L. (1978) The effects of root shape and biology on bone growth. *Journal of Periodontology* **49**, 33–35.

Nalbandian, J. & Helldén, L. (1982) Response of the periodontal tissues of the beagle dog to polytetrafluoroethylene implants. *Oral Surgery, Oral Medicine, Oral Pathology* **54**, 452–460.

Nielsen, I. M., Ellegaard, B. & Karring, T. (1980) Kielbone® in healing interradicular lesions in monkeys. *Journal of Periodontal Research* **15**, 328–337.

Noyes, F. R., Barber, S. D. & Mangine, R. E. (1990) Bone-patellar ligament-bone and fascia lata allografts for reconstruction of the anterior cruciate ligament. *Journal of Bone and Joint Surgery – American Volume* **72A**, 1125–1136.

Nyman, S., Gottlow, J., Karring, T. & Lindhe, J. (1982) The regenerative potential of the periodontal ligament. An experimental study in the monkey. *Journal of Clinical Periodontology* **9**, 257–265.

Pettersson, E. C. & Aukhil, I. (1986) Citric acid conditioning of roots affects guided tissue regeneration in experimental periodontal wounds. *Journal of Periodontal Research* **21**, 543–552.

Piattelli, A., Scarano, A., Corigliano, M. & Piatelli, M. (1996) Comparison of bone regeneration with the use of mineralized and demineralized freeze-dried bone allografts: a histological and histochemical study in man. *Biomaterials* **17**, 1127–1131.

Prolo, D. J., Pedrotti, P. W., Burres, K. P. & Oklund, S. (1982) Superior osteogenesis in transplanted allogeneic canine skull following chemical sterilization. *Clinical Orthopaedics and Related Research* **168**, 230–242.

Reynolds, M. & Bowers, G. M. (1996) Fate of demineralized freeze-dried bone allografts in human intrabony defects. *Journal of Periodontology* **67**, 150–157.

Roberts, T. S., Drez, D. Jr., McCarthy, W. & Paine, R. (1991) Anterior cruciate ligament reconstruction using freeze-dried, ethylene oxide-sterilized, bone-patellar tendon-bone allografts. Two year results in thirty-six patients. *Americal Journal of Sports Medicine* **19**, 35–41.

Schaffer, E. M. (1957) Cementum and dentine implants in a dog and a rhesus monkey. *Journal of Periodontology* **28**, 125–131.

Schenk, R. K. (1994) Bone regeneration: biologic basis. In: *Guided Bone Regeneration in Implant Dentistry*, eds. Buser, D., Dahlin, C & Schenk, R. K., pp. 49–100. Chicago: Quintessence Publishing Co., Inc.

Schmitz, J. P. & Hollinger, J. O. (1986) The critical size defect as an experimental model for craniomandibulofacial nonunions. *Clinical Orthopaedics and Related Research* **205**, 299–308.

Schwartz, Z., Mellonig, J. T., Carnes, D. L. Jr., de la Fontaine, J., Cochran, D. L., Dean, D. D. & Boyan, B. D. (1996) Ability of commercial demineralized freeze-dried bone allograft to induce new bone formation. *Journal of Periodontology* **67**, 918–926.

Schwartz, Z., Somers, A., Mellonig, J. T., Carnes, D. L. Jr., Dean, D. D., Cochran, D. L. & Boyan, B. D. (1998a) Ability of commercial demineralized freeze-dried bone allograft to induce new bone formation is dependent on donor age but not gender. *Journal of Periodontology* **69**, 470–478.

Schwartz, Z., Somers, A., Mellonig, J. T., Carnes, D. L. Jr., Wozney, J. M., Dean, D. D., Cochran, D. L. & Boyan, B. D. (1998b) Addition of human recombinant BMP-2 to inactive commercial human DFDBA makes it an effective composite bone inductive implant material. *Journal of Periodontology* **69**, 1337–1345.

Scopp, I., Kassouny, D. & Morgan, F. (1966) Bovine bone (Boplant). *Journal of Periodontology* **37**, 400–407.

Tshamala, M., Cox, E., De Cock, J., Goddeeris, B. M. & Mattheeuws, D. (1999) Antigenicity of cortical bone allografts in dogs and effect of ethylene oxide sterilization. *Veterinary Immunology and Immunopathology* **69**, 47–59.

Urist, M. R. (1965) Bone formation by autoinduction. *Science* **150**, 893–899.

Urist, M. R. (1994) The search for and the discovery of bone morphogenic protein (BMP). In: *Bone Grafts, Derivatives and Substitutes*, eds. Urist, M. R., O'Connor., B. T. & Burswell, R. G., pp. 315–362. Oxford: Butterworth-Heinemann Ltd.

Urist, M. R., Silverman, B. F., Büring, K., Dubuc, F. L. & Rosenberg, J. M. (1967) The bone induction principle. *Clinical Orthopaedics* **53**, 243–283.

Wikesjö, U. M. E., Kean, C. J. C. & Zimmerman, G. J. (1994) Periodontal repair in dogs: supraalveolar defect models for evaluation of safety and efficacy of periodontal reconstructive therapy. *Journal of Periodontology* **65**, 1151–1157.

Zhang, Q., Cornu, O. & Delloye, C. (1997) Ethylene oxide does not extinguish the osteoinductive capacity of demineralized bone. A reappraisal in rats. *Acta Orthopaedica Scandinavia* **68**, 104–108.

Address:
Morten Klepp
Solakrossen 14
4050 Sola, Norway
Fax: +47 51 65 05 50
E-mail: morten.klepp@stavanger.online.no